Vivoni Enrique (Orcid ID: 0000-0002-2659-9459)
Scott Russell (Orcid ID: 0000-0003-2987-5380)

Long-term Research Catchments to Investigate Shrub Encroachment in the Sonoran and Chihuahuan Deserts: Santa Rita and Jornada Experimental Ranges

Enrique R. Vivoni[1,2,*], Eli R. Pérez-Ruiz[2,3], Zachary T. Keller[2], Eric A. Escoto[2], Ryan C. Templeton[1], Nolie P. Templeton[1], Cody A. Anderson[1], Adam P. Schreiner-McGraw[2,8], Luis A. Méndez-Barroso[2,4], Agustin Robles-Morua[2,4], Russell L. Scott[5], Steven R. Archer[6], and Debra P.C. Peters[7]

1. School of Sustainable Engineering and the Built Environment, Arizona State University, Tempe, AZ, USA, 85287.

2. School of Earth and Space Exploration, Arizona State University, Tempe, AZ, USA, 85287.

3. Departamento de Ingeniería Civil y Ambiental, Universidad Autónoma de Ciudad Juárez, Ciudad Juárez, Chihuahua, México.

4. Departamento de Ciencias del Agua y Medioambiente, Instituto Tecnológico de Sonora, Ciudad Obregón, Sonora, México.

5. USDA-ARS Southwest Watershed Research Center, 2000 E. Allen Road, Tucson, AZ, USA, 85719.

6. School of Natural Resources and the Environment, University of Arizona, Tucson, AZ, USA, 85721.

7. USDA-ARS Jornada Experimental Range, 2995 Knox St., Las Cruces, NM, USA, 88003.

8. Department of Environmental Sciences, University of California Riverside, Riverside, CA, USA, 92521

Running Head: *SRER and JER Research Catchments*
Revised for *Hydrological Processes*, #HYP-20-0878.R1
Data Note – Special Issue on Research and observatory catchments
December 27, 2020

* *Corresponding author address:* Enrique R. Vivoni, School of Earth and Space Exploration, ISTB4, Room 769, Arizona State University, Tempe, AZ, 85287-6004, tel: 480-727-3575, fax: 480-965-8102, email: vivoni@asu.edu.

Abstract

Woody plant encroachment is a global phenomenon whereby shrubs or trees replace grasses. The hydrological consequences of this ecological shift are of broad interest in ecohydrology, yet little is known of how plant and intercanopy patch dynamics, distributions, and connectivity influence catchment-scale responses. To address this gap, we established research catchments in the Sonoran and Chihuahuan Deserts (near Green Valley, Arizona and near Las Cruces, New Mexico, respectively) that represent shrub encroachment in contrasting arid climates. Our main goals in the coordinated observations were to: (1) independently measure the components of the catchment water balance, (2) deploy sensors to quantify the spatial patterns of ecohydrological processes, (3) use novel methods for characterizing catchment properties, and (4) assess shrub encroachment impacts on ecohydrological processes through modeling studies. Datasets on meteorological variables; energy, radiation, and CO_2 fluxes; evapotranspiration; soil moisture and temperature; and runoff at various scales now extend to nearly 10 years of observations at each site, including both wet and dry periods. Here, we provide a brief overview of data collection efforts and offer suggestions for how the coordinated datasets can be exploited for ecohydrological inferences and modeling studies. Given the representative nature of the catchments, the available databases can be used to generalize findings to other catchments in desert landscapes.

Keywords: water balance, ecohydrology, arid hydrology, eddy covariance technique, instrument networks, hydrological modeling.

1. Data Set Name

Hydrologic data from long-term research catchments at the Santa Rita and Jornada Experimental Ranges

2. Introduction and Site Descriptions

Woody plant encroachment is a global phenomenon whereby shrubs or trees replace grasses (Archer et al., 2017). The ecohydrological consequences of this vegetation change have been studied primarily in arid and semiarid sites where hydrological processes are dominated by vertical exchanges (e.g., Huxman et al., 2005). Catchment-scale perspectives are limited and typically confined to short periods that do not adequately capture the range of inter- to intra-annual hydrological variability. To address this gap, we established research catchments with similar instrument networks in the Sonoran and Chihuahuan Deserts to investigate hydrological processes resulting from long-term increases in the amount and distribution of shrubs in areas historically dominated by perennial grasses (McClaran, 2003; Gibbens et al., 2005). Fig. 1 shows the location of the research catchments in the southwestern United States – Santa Rita Experimental Range (SRER, 31.817° N, -110.851° W, ~1200 m) in southern Arizona and Jornada Experimental Range (JER, 32.585° N, -106.603° W, ~1500 m) in southern New Mexico.

The SRER consists of two watersheds (Fig. 1b) totaling 2.18 hectares in area upstream of two Santa Rita-type flumes (Smith et al., 1981) established in 1976 by the USDA-ARS Southwest Watershed Research Center (Polyakov et al., 2010). Located on a piedmont slope extending from the Santa Rita mountains, the climate conditions are considered as Köppen classification BSh (hot, semiarid, Beck et al., 2018). While Sonoran Desert grasses were previously dominant (McClaran, 2003), the area is now a savanna of velvet mesquite (*Prosopis velutina*) arborescents in a matrix of perennial C4 bunchgrasses (e.g., black grama, *Bouteloua*

eriopoda) and succulents (e.g., prickly pear, *Opuntia engelmannii*). Drainage on the active alluvial fan terrace occurs in small ephemeral channels (<0.5 m width) with sandy bottoms, while hillslope soils are deep and with sandy clay and sandy clay loam textures.

The JER is a single watershed (Fig. 1c) of 4.67 hectares in area upstream of a similar Santa Rita-type outlet flume installed in 1977 (Tromble, 1998). The catchment is on a piedmont slope emanating from the San Andres mountains (Schreiner-McGraw and Vivoni, 2018). Climate at the site has a Köppen classification of BWk (cold, desert) typical of the Chihuahuan Desert. Gibbens et al. (2005) described the area as a grassland prior to 1860, whereas a mixed shrubland composed of creosotebush (*Larrea tridentata*), honey mesquite (*Prosopis glandulosa*), and mariola (*Parthenium incanum*) is present today (Templeton et al., 2014). Drainage in the remnant alluvial fan flows into a main channel (0.5 to 1 m width) from hillslopes whose soils are shallow (< 0.5 m) due to a $CaCO_3$ horizon and sandy loam in texture. Bare soils occupy 65% of the catchment and contain large amounts of surface rock.

The two settings have well established differences that offer novel insights into the ecohydrological processes of arid and semiarid regions. At the lower elevation SRER, the warmer and wetter Sonoran Desert conditions are linked to a more pronounced North American monsoon (Adams and Comrie, 1997) which brings summer precipitation to the region. At the higher elevation JER, the colder and drier Chihuahuan Desert conditions lead to lower vegetation cover with shorter statured shrub species and greater amounts of bare soil. Important differences also are present in soils with shallower and rockier areas of higher slope at JER.

At the two sites, long-term precipitation and outlet streamflow data are available from the USDA-ARS (SRER: http://www.tucson.ars.ag.gov/dap/; JER: http://lter.jornada.nmsu.edu/data-catalog/) at daily or greater resolution since the late 1970s, with some missing periods. This data

availability and the supporting infrastructure at SRER and JER motivated the expansion of the instrument network, as described in the following section, to establish two coordinated research catchments. Each site included an eddy covariance (EC) tower whose sub-daily data products are distributed separately through AmeriFlux at http://ameriflux.lbl.gov/sites/siteinfo/US-SRS (SRER) and http://ameriflux.lbl.gov/sites/siteinfo/US-Jo2 (JER). The locations also afforded the opportunity to establish instrument test beds, where traditional sensors are compared to novel methods, for instance, to estimate soil moisture (cosmic ray neutron sensor, CRNS, Schreiner-McGraw et al., 2016) and precipitation (disdrometer, Tokay et al., 2014). To date, cross-site instrument networks have been compared in terms of their soil moisture and temperature distributions (Mascaro and Vivoni, 2016), the link between soil conditions and turbulent fluxes (Anderson and Vivoni, 2016), and the water balance closure (Schreiner-McGraw et al., 2016).

3. Methods and Data Description

The instrument networks shown in Fig. 1 were deployed in May 2010 (JER) and May 2011 (SRER) using a coordinated approach to measure water, energy, and CO_2 states and fluxes. The water balance approach ($dSM/dt = P - ET - Q$, where SM is soil moisture, P is precipitation, ET is evapotranspiration, and Q is outlet streamflow) was emphasized in the instrument network design (Templeton et al., 2014). Tipping-bucket rain gauges (TE525, Texas Electronics, Dallas, TX, USA; resolution 0.2 mm, accuracy of ±1%) and line transects of dielectric impedance soil moisture sensors (Hydra Probe II, Stevens Water, Portland, OR, USA; accuracy of 0.01 m^3/m^3) arranged over depth profiles (5, 15, and 30 cm) were deployed to obtain spatially-averaged estimates of SM and P (Fig. 1b, c). The Santa Rita-type outlet flumes were equipped with pressure transducers (CS450, Campbell Scientific, Logan, UT, USA; resolution of 0.0035% full scale, accuracy of ±0.1% full scale) to estimate water depths through a linear relation after which

Q values were obtained following Smith et al. (1981). The EC method (Baldocchi et al., 1998) was implemented to obtain *ET* through the installation of a 10-m meteorological flux tower at each site. Tower sensors included a net radiometer (CNR2, Kipp & Zonen, Delft, The Netherlands; accuracy of ±10% daily value), a three-dimensional sonic anemometer (CSAT3, Campbell Scientific, Logan, UT, USA; resolution of 0.5 to 1 mm/s; accuracy of ±4 to 8 cm/s offset error), an open-path infrared gas analyzer (LI7500, LI-COR, Lincoln, NE, USA; accuracy of ±1% for CO_2 and ±2% for H_2O), and soil heat flux plates (HPF01, Hukseflux, Delft, The Netherlands; accuracy of ±3%). *ET* is obtained as the covariance between high-frequency turbulent fluctuations in vertical wind velocity and H_2O concentration. Energy balance closure errors for *ET* estimates range from 10 to 15% of the available energy at the two sites. Analyses of the EC footprint indicate that spatial scales similar to that of the instrument networks are achieved (Vivoni et al., 2014). Pierini et al. (2014) and Templeton et al. (2014) provide a full description of the instrument network at SRER and JER, respectively, as summarized in Table 1, including the spatial patterns obtained from the distributed measurements of *P* and *SM*.

After installation of the instrument networks, in-situ calibrations were carried out for all sensors following manufacturer guidelines (Templeton et al., 2014; Pierini et al., 2014). Site maintenance was performed on a nearly monthly basis in the research catchments over the study periods (2011-2018 at SRER; 2010-2019 at JER). Frequent visits allowed for troubleshooting and quality control of measurement techniques, with annual sensor re-calibrations performed for the EC method sensors. All measurements were obtained at high temporal resolutions (e.g., 1-min for *Q* and *P*; 20 Hz for EC sensors) and aggregated to a common resolution of 30-min for quality control purposes. Data processing included the removal of values exceeding specified ranges and use of standard filtering techniques for EC measurements (Pérez-Ruiz et al., 2020).

Data gaps due to instrument failures, power issues, or values removed due to poor quality were identified at the 30-min resolution for each sensor. Where possible, we used information from nearby sensors to fill gaps, thus obtaining daily values aggregated to the catchment scale with valid measurements only; otherwise, a No Data value (-9999) was reported.

The dataset released here consists of water, energy, and CO_2 fluxes aggregated to a daily resolution and commensurate with a spatial scale similar to the research catchments. These observations allow cross-site comparisons at inter- to intra-annual time scales. The EC method is also used to obtain the energy balance ($R_n - G = H + \lambda ET$, where R_n is net radiation, G is ground heat flux, H is sensible heat flux, and λET is latent heat flux), using ancillary measurements, as described in Templeton et al. (2014). Similarly, the EC method quantifies CO_2 fluxes between ecosystems and the atmosphere ($NEE = R_{eco} - GPP$, where NEE is net ecosystem exchange, R_{eco} is ecosystem respiration, and GPP is gross primary productivity), as described in Pérez-Ruiz et al. (2020). Temporal aggregations were performed through daily totals for P, ET, and Q in units of mm/day and daily averages for SM (m^3/m^3); R_n, H, and λET (W/m^2); and NEE, GPP, and R_{eco} (g CO_2/m^2/day). Spatial aggregations consisted of Thiessen polygon averaging of P data and arithmetic averaging of depth-averaged SM measurements available each day. Aggregations to the daily resolution at the scale of the research catchments during the study periods allow assessments and comparisons to remotely-sensed observations, as well as support hydrological modeling efforts (e.g., Pierini et al., 2014; Schreiner-McGraw and Vivoni, 2018).

4. Cross-Site Comparison at Inter- to Intra-Annual Scales

Table 1 compares the annual water and energy balance components at the SRER and JER research catchments obtained over the complete years in the periods of record. The ET/P ratio is close to unity at both sites (1.04 ± 0.22 at SRER; 0.98 ± 0.26 at JER), indicating a majority of the

P input is returned to the atmosphere during a year as *ET*, when averaged over the period of record. Inter-annual variability of the water fluxes, however, is particularly high. For example, coefficients of variations (CV = σ/μ, where σ is annual standard deviation and μ is the annual average) for outlet streamflow (*Q*) are 0.90 and 0.67 at SRER and JER, respectively. As expected at the annual scale, the change in *SM* is small, though inter-annual variability is high due to carry-over effects during wet years. Due to the arid and semiarid climate, the majority of net radiation input is partitioned into sensible heat flux, with H/R_n values of 0.58 ± 0.14 at SRER and 0.57 ± 0.05 at JER, respectively. As a result of the climatic conditions, the Bowen Ratio ($B = H/\lambda ET$) is above unity (1.79 ± 0.25 and 2.95 ± 0.54 at SRER and JER, respectively), with higher CVs for λET due to high inter-annual variations in water availability.

The water, energy, and CO_2 fluxes in the research catchments are compared at the intra-annual (monthly) time scale in Fig. 2. The higher *P* at SRER has a more marked seasonality during the North American monsoon (July to September), leading to a more pronounced seasonality in both *ET* and *Q*. At both sites, the one-month delay in maximum seasonal *ET* with respect to maximum *P* reflects the time required for quiescent grasses and shrubs to green-up during the monsoon (Vivoni et al., 2008). While elevation-mediated differences are noted in R_n, the intra-annual variability of energy partitioning depends largely on water availability. Summer months at SRER have λET that exceed *H*, but this is not observed at JER. Water and energy fluxes are strongly linked to the ecosystem CO_2 response, which exhibit stark differences in *GPP* and *NEE* during the monsoon and subsequent autumn season. Higher summer-time moisture and temperature conditions at SRER enhance its carbon uptake (more negative *NEE*) relative to JER, consistent with its higher aboveground biomass and less bare soil.

5. Data Availability

Datasets for the research catchments at SRER and JER are publicly available in Zenodo in the form of an Excel spreadsheet with metadata (Vivoni et al., 2020). Data processing of the water, energy, and CO_2 observations included aggregation to the daily resolution and spatial averaging, where appropriate, and can be used to reproduce monthly and annual balances. For ancillary datasets, geospatial layers or higher-resolution observations, please contact Enrique R. Vivoni (Enrique.Vivoni@asu.edu, Principal Investigator of SRER and JER Research Catchments project) who also serves as a contact for potential collaborations. Data collection is on-going beyond the period provided in this release and expected to be updated on an annual basis.

6. Funding, Contributors, and Data Ownership

This research was supported by funding from the U.S. Army Research Office (56059-EV-PCS), National Science Foundation (DEB-0618210, DEB-1832194) through the Jornada Long-term Ecological Research Program, and U.S. Department of Agriculture (2015-67019-23314). Data collection at JER was primarily carried by Ryan C. Templeton (2010-2011), Cody A. Anderson (2011-2013), Adam P. Schreiner-McGraw (2012-2016), Eli R. Pérez-Ruiz (2016-2019), and Zachary T. Keller (2019-2020). Data collection at SRER was performed by Nolie P. Templeton (2011-2016), Cody A. Anderson (2011-2013), Adam P. Schreiner-McGraw (2012-2016), and Eli R. Pérez-Ruiz (2016-2020). Additional field installation, maintenance and support was provided by Enrique R. Vivoni, Luis A. Mendez-Barroso, Agustin Robles-Morua, and Eric A. Escoto. We thank the SRER and JER for site access and instrumentation support. Datasets were assembled by Eli R. Perez-Ruiz and Enrique R. Vivoni (Principal Investigator) for this release, shared under a Creative Commons Attribution 4.0 International Public License, and must be appropriately cited for their use (Vivoni et al., 2020).

References

Adams, D. K., and A. C. Comrie (1997), The North American Monsoon, *Bull. Amer. Meteorol. Soc.*, *78*(10), 2197 – 2213.

Anderson, C. A., and E. R. Vivoni (2016), Land surface states within the flux footprint impact land-atmosphere coupling in two semiarid ecosystems of the southwestern U.S., *Water Resour. Res.*, *52*, 4785 – 4800.

Archer, S. R., E. M. Andersen, K. I. Predick, S. Schwinning, R. J. Steidl, and S. R. Woods (2017), Woody plant encroachment: causes and consequences. pp 25-84. In: Briske, D. D. (ed). *Rangeland Systems: Processes, Management and Challenges*. Cham, Switzerland: Springer. 661 pp.

Baldocchi, D., B. B. Hicks, and T. P. Meyers (1988), Measuring biosphere-atmosphere exchanges of biologically related gases with micrometeorological method, *Ecology*, *69*, 1331 – 1340.

Beck, H. E., N. E. Zimmermann, T. R. McVicar, N. Vergopolan, A. Berg, and E. F. Wood (2018), Present and future Koppen-Geiger climate classification at 1-km resolution, *Scientific Data*, *5*, 180214, https://doi.org/10.1038/sdata.2018.214.

Gibbens, R. P., R. P. McNeely, K. M. Havstad, R. F. Beck, and B. Nolen (2005), Vegetation changes in the Jornada basin from 1858 to 1998, *J. Arid Environ.*, *61*, 651 – 668.

Huxman, T. E., B. P. Wilcox, D. D. Breshears, R. L. Scott, K. A. Snyder, E. E. Small, K. Hultine, W. T. Pockman, and R. B. Jackson (2005), Ecohydrological implications of woody plant encroachment, *Ecology*, *86*(2), 308 – 319.

Mascaro, G., and E. R. Vivoni (2016), On the observed hysteresis in field-scale soil moisture variability and its physical controls, *Environ. Res. Lett.*, *11*(8), 084008, https://doi.org/10.1088/1748-9326/11/8/084008.

McClaran, M. P. (2003), *A century of vegetation change on the Santa Rita Experimental Range, in Santa Rita Experimental Range: 100 years (1903 to 2003) of accomplishments and contributions*, pp. 16 – 33, U.S. Department of Agriculture, Forest Service, Rocky Mountain Research Station, Tucson, AZ.

Pérez-Ruiz, E. R., E. R. Vivoni, and N. P. Templeton (2020), Urban land cover type determines the sensitivity of carbon dioxide fluxes to precipitation in Phoenix, Arizona, *PLOS One*, *15*(2), e0228537. https://doi.org/10.1371/journal.pone.0228537.

Pierini, N. A., Vivoni, E. R., Robles-Morua, A., Scott, R. L., and M. A. Nearing (2014), Using observations and a distributed hydrologic model to explore runoff threshold processes linked with mesquite encroachment in the Sonoran Desert, *Water Resour. Res.*, *50*(10), 8191 – 8215.

Polyakov, V. O., M. A. Nearing, M. H. Nichols, R. L. Scott, J. J. Stone, and M. P. McClaran (2010), Long-term runoff and sediment yields from small semiarid watersheds in southern Arizona, *Water Resour. Res.*, *46*(9), W09512, doi:10.1029/2009WR009001.

Schreiner-McGraw, A. P., and E. R. Vivoni (2017), Percolation observations in an arid piedmont watershed and linkages to historical conditions in the Chihuahuan Desert, *Ecosphere*, *8*(11), e02000. https://doi.org/10.1002/ecs2.2000.

Schreiner-McGraw, A. P., and E. R. Vivoni (2018), On the sensitivity of hillslope runoff and channel transmission losses in arid piedmont slopes, *Water Resour. Res.*, *54*(7), 4498 – 4518.

Schreiner-McGraw, A. P., E. R. Vivoni, G. Mascaro, and T. E. Franz (2016), Closing the water balance with cosmic-ray soil moisture measurements and assessing their relation with evapotranspiration in two semiarid watersheds, *Hydrol. Earth Sys. Sci.*, *20*, 329 – 345.

Smith, R. E., D. L. Chery, K. G. Renard, and W. R. Gwinn (1981), *Supercritical flow flumes for measuring sediment-laden flow*, Tech. Bull. 1655, 70 pp., Washington, D.C.

Templeton, R. C., E. R. Vivoni, L. A. Méndez-Barroso, N. A. Pierini, C. A. Anderson, A. Rango, A. S. Laliberte, and R. L. Scott (2014), High-resolution characterization of a semiarid watershed: Implications on evapotranspiration estimates, *J. Hydrol.*, *509*, 306 – 319.

Tokay, A., D. B. Wolff, and W. A. Petersen (2014), Evaluation of the new version of the laser-optical disdrometer, OTT Parsivel^2, *J. Atmos. Oceanic Technol.*, *31*, 1276 – 1288.

Tromble, J. M. (1988), Water budget for creosotebush-infested rangeland, *J. Arid Environ.*, *15*, 71–74.

Vivoni, E. R., A. Rango, C. A. Anderson, N. A. Pierini, A. P. Schreiner-McGraw, S. Saripalli, and A. S. Laliberte (2014), Ecohydrology with unmanned aerial vehicles, *Ecosphere*, *5*(10), art130, http://dx.doi.org/10.1890/ES14-00217.1.

Vivoni, E. R., H. A. Moreno, G. Mascaro, J. C. Rodriguez, C. J. Watts, J. Garatuza-Payan, and R. L. Scott (2008), Observed relation between evapotranspiration and soil moisture in the North American monsoon region, *Geophys. Res. Lett.*, *35*, L22403, doi:10.1029/2008GL036001.

Vivoni, E. R., E. R. Pérez-Ruiz, Z. T. Keller, E. A. Escoto, A. P. Schreiner-McGraw, N. P. Templeton, C. A. Anderson, and R. C. Templeton (2020), Hydrologic data from long-term research catchments at the Santa Rita and Jornada Experimental Ranges (Version 2), Zenodo, https://zenodo.org/record/4290771.

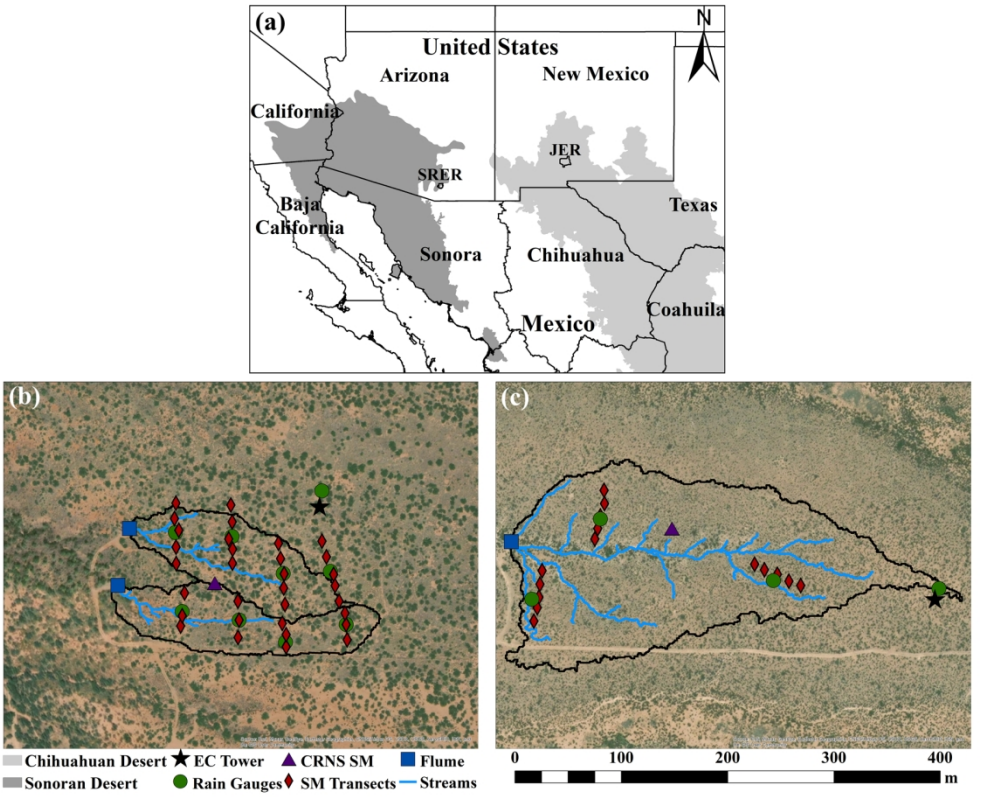

Research catchments in the southwestern United States. (a) Locations of Santa Rita Experimental Range (SRER, Arizona) and Jornada Experimental Range (JER, New Mexico) in the Sonoran and Chihuahuan Deserts, respectively. Watershed boundaries (black polygons), drainage networks (blue lines labeled streams), and instrument locations at: (b) SRER (2.18 ha total, 31.817° N, -110.851° W, 1169 m) and (c) JER (4.67 ha, 32.585° N, -106.603° W, 1469 m) on the ESRI World Imagery basemap (Sources: Esri, DigitalGlobe, GeoEye, i-cubed, USDA FSA, USGS, AEX, Getmapping, Aerogrid, IGN, IGP, swisstopo, and the GIS User Community).

SRER

JER

(a)

(b)

(c)

(d)

(e)

(f)

R_n

H

λET

GPP

R_{eco}

NEE

ET (mm month^{-1})

P (mm month^{-1})

Q (mm month^{-1})

Energy fluxes (W m^{-2})

Carbon Fluxes (g CO_2 m^{-2} month^{-1})

J F M A M J J A S O N D

Month

Long-term monthly values of water, energy, and CO_2 fluxes at the SRER (left) and JER (right) research catchments. (a, b) Precipitation (*P*), evapotranspiration (*ET*), and outlet streamflow (*Q*). (c, d) Net radiation (R_n), sensible heat flux (*H*), and latent heat flux (λET). (e, f) Gross primary productivity (*GPP*), ecosystem respiration (R_{eco}), and net ecosystem exchange (*NEE*). Symbols represent monthly averages and error bars depict ±1 monthly standard deviation over the entire study periods: SRER (2011-2018) and JER (2010-2019). Due to low values (Table 1), *dSM/dt* and *G* have been omitted from (a, b) and (c, d), respectively.

	Complete Years	Sensors	Annual Average and Standard Deviation
SRER			
Water Components (mm yr^{-1})			
Precipitation (*P*)	2012-2018	TE-525, Texas Instruments	406 ± 78
Evapotranspiration (*ET*)	2012-2018	LI-7500, LI-COR; CSAT3, Campbell Sci.	421 ± 39
Streamflow (*Q*)	2012-2018	Outlet flume; CS450 pressure, Campbell Sci.	30 ± 27
Soil Moisture (*SM*) Change	2012-2018	Hydra Probe II, Stevens	2 ± 26
Energy Components (W m^{-2})			
Net Radiation (R_n)	2012-2018	CNR2, Kipp & Zonen	105 ± 23
Latent Heat Flux (λET)	2012-2018	LI-7500, LI-COR; CSAT3, Campbell Sci.	34 ± 4
Sensible Heat Flux (*H*)	2012-2018	CSAT3, Campbell Sci.	61 ± 5
Ground Heat Flux (*G*)	2012-2018	HFP01, Hukseflux	1 ± 2
JER			
Water Components (mm yr^{-1})			
Precipitation (*P*)	2011-2019	TE-525, Texas Instruments	285 ± 51
Evapotranspiration (*ET*)	2011-2019	LI-7500, LI-COR; CSAT3, Campbell Sci.	280 ± 55
Streamflow (*Q*)	2011-2019	Outlet flume; CS450 pressure, Campbell Sci.	9 ± 6
Soil Moisture (*SM*) Change	2011-2019	Hydra Probe II, Stevens	1 ± 20
Energy Components (W m^{-2})			
Net Radiation (R_n)	2011-2019	CNR2, Kipp & Zonen	114 ± 10
Latent Heat Flux (λET)	2011-2019	LI-7500, LI-COR; CSAT3, Campbell Sci.	22 ± 4
Sensible Heat Flux (*H*)	2011-2019	CSAT3, Campbell Sci.	65 ± 2
Ground Heat Flux (*G*)	2011-2019	HFP01, Hukseflux	6 ± 13